Coronary Microcirculatory Dysfunction in Aortic Stenosis

K Rajappan, O Rimoldi, DJ Pennell, PG Camici, DJ Sheridan

Academic Cardiology Unit, MRC Clinical Sciences Centre, and Cardiovascular Magnetic Resonance Unit, Imperial College School of Medicine, London, UK

Abstract

Development of left ventricular hypertrophy (LVH) in aortic stenosis (AS) is accompanied by dysfunction of the coronary microcirculation, demonstrated by an impaired coronary vasodilator reserve (CVR), but the relative contribution of LVH and changes in haemodynamics remains unclear. In twenty patients with AS, an increase in resting myocardial blood flow (MBF), assessed with positron emission tomography, was demonstrated, proportional to hypertrophy measured with cardiac magnetic resonance, presumably as a result of coronary autoregulation. However, an inverse relationship between CVR and echocardiographic peak transvalvular pressure gradient and left ventricular pressure multiplied by heart rate (LVRPP) suggests that the effect of haemodynamic and intramural forces may be to counteract autoregulation, maintaining transmural MBF at rest, but impairing the coronary microcirculation stress response, particularly within the subendocardium.

1. Introduction

Left ventricular hypertrophy (LVH) in patients with aortic valve stenosis (AS) is an adaptive response, which attempts to reduce wall stress in the left ventricle. However, the resulting increase in myocardial mass requires a proportional change in the blood flow to maintain a *status quo* between demand and supply. Eventually, there is a transition from a physiological response to the increased workload, to a pathological state where maintenance of resting blood flow, through coronary autoregulation, consumes coronary reserve capacity. This is often associated with symptoms suggestive of myocardial ischaemia, despite angiographically normal coronary arteries. [1]

Microcirculatory dysfunction has been implicated as a possible cause of this phenomenon, and a reduced coronary vasodilator reserve (CVR), an index of the functional capacity of the coronary microcirculation, has previously been demonstrated in such patients. [2] Available evidence suggests that several factors contribute to this: structural remodelling of the intramyocardial coronary arterioles leading to an increase in wall:lumen ratio; a reduction in the number of resistance vessels; and systolic impedance to coronary flow as a result of perivascular compression. [3] Furthermore, electrocardiographic findings in these patients may include ST/T wave changes compatible with subendocardial ischaemia, suggesting regional variation in microcirculatory function, with more severe impairment in the subendocardial layer.

Recent advances in positron emission tomography (PET) scanner technology [4] make it possible to study the transmural distribution of myocardial blood flow (MBF) and variation in microcirculatory function. The aim of the present study, therefore, was to determine the relative effect of changes in left ventricular mass (LVM) and haemodynamics on the subendocardial and subepicardial coronary microcirculation in patients with AS and angiographically normal epicardial arteries using echocardiography, cardiac magnetic resonance (CMR), and PET with oxygen-15 labelled water ($H_2{}^{15}O$).

2. Methods

2.1. Study Group

Twenty patients were studied (16 men), aged 66 ± 10 years. All had a peak transvalvular gradient of over 50 mmHg (either with echocardiography or at cardiac catheterisation), no more than minimal aortic regurgitation (grade ≤1/4), angiographically normal coronary arteries, systolic blood pressure less than 160 mmHg, and diastolic blood pressure less than 90 mmHg. Others were excluded if they had asthma, as this precluded use of dipyridamole, or if they were taking β-blocker, ACE inhibitor, calcium channel blocker, or diuretic therapy.

The Research and Ethics Committees approved the study, and the subjects gave informed, written consent. All procedures were carried out in accordance with local institutional guidelines. Radiation exposure was licensed by the UK Administration of Radioactive Substances Advisory Committee (ARSAC).

0276-6547/01 $17.00 © 2001 IEEE

Computers in Cardiology 2001;28:289-292.

2.2 Echocardiography

Transthoracic echocardiography was performed using an ATL HDI 3000 cardiac ultrasound scanner, according to the guidelines of the American Society of Echocardiography. [5] Left ventricular dimensions were measured at end diastole by 2-D echocardiography, and continuous wave Doppler was used to derive the peak transvalvular pressure gradient across the aortic valve (peak AVG). [6] All echocardiographic values were the mean of three separate readings.

2.3. Cardiac magnetic resonance

LV function and LVM were assessed using a Picker Edge 1.5-T scanner (Picker, Cleveland, OH) with electrocardiographic (ECG) triggering and a standard body coil. The cardiac short axis was determined form three scout images. The initial transaxial scout was used to define a line from the left ventricular apex to the centre of the mitral valve, the vertical long axis (VLA) scout. The horizontal long axis (HLA) scout was aligned through the apex and mitral valve on the VLA scout image. A diastolic image at end expiration on the HLA image provided the reference image on which short axis (SA) slices were positioned. Contiguous 10 mm SA slices were acquired during a single breathold using a segmented gradient-echo Turbo-FLASH sequence, and end-diastolic volume (EDV), end-systolic volume (ESV), ejection fraction (EF) and LVM were calculated as previously described. [7] Image analysis was performed on a personal computer using software developed in-house (RGBwin).

2.4. Positron emission tomography

The studies were performed on an ECAT EXACT 3D positron tomograph (CTI, Knoxville, TN) with an axial field of view of 23.4 cm. [4] All subjects abstained from caffeine-containing drinks for 24 hours prior to the PET scan. Before performing the emission study, a single photon point source filled with 150 MBq of ^{137}Cs was used for transmission data acquisition. The transmission scan was recorded for 10 minutes to measure the attenuation correction coefficients to be used for each line of response of the emission sinogram. After the transmission scan, MBF was measured at baseline using approximately 1.3 MBq/kg of $H_2{}^{15}O$ injected intravenously. Scanning commenced at the start of build up of $H_2{}^{15}O$ activity (2 minutes prior to injection) and continued for 12 minutes. Data were acquired in list mode, recording up to 4 million coincidences/second with approximately 190 million lines of response. This allowed high temporal sampling, flexible frame rebinning post hoc, and flexibility for iterative image reconstruction routines. After allowing 3 minutes for decay, intravenous dipyridamole (0.56mg/kg over 4 minutes) was used to achieve near maximal coronary vasodilatation, and a repeat MBF measurement was carried out. Blood pressure and 12-lead electrocardiograms were recorded every three minutes during the baseline scan, and every minute from the start of dipyridamole infusion for 15 minutes.

The sinograms obtained were corrected for attenuation and reconstructed by dedicated array processors and a reprojection reconstruction algorithm using a Hann filter (Nyquist cut-off). This allows a spatial resolution of 6 mm full width half-maximum to be achieved. [4] Fourier rebinned images were then transferred to a SUN Ultra 10 work station (Sun Microsystems, Mountain View, CA, USA) for further analysis. To define regions of interest, myocardial and blood pool images were generated using a combination of factor and cluster analysis to generate factor images. All images were resliced in the short axis, and LV myocardium, left atrium, and right ventricular regions of interest (ROIs) drawn and projected onto the dynamic $H_2{}^{15}O$ images to generate tissue, arterial blood, and venous blood time activity curves respectively. Tissue and arterial activity curves were fitted to a single tissue compartment tracer kinetic model to give values of MBF (ml/g/min). [8]

To determine differences between subendocardial and subepicardial MBF the LV myocardial ROIs were divided by a central line, and a model for MBF, which accounts for spillover from subendocardium to subepicardium was used. CVR was calculated as the ratio of hyperaemic MBF (following dipyridamole) to resting MBF. This was done for the subendocardial and subepicardial regions separately, as well as for the myocardium transmurally.

To calculate ventricular blood flow (ml/min) the MBF (ml/min/g) measured was multiplied by LVM assessed by CMR.

In the normal human heart oxygen consumption is linearly related to the rate-pressure product (RPP), an index of external cardiac work, and both are related to coronary blood flow. In patients with significant aortic stenosis and left ventricular hypertrophy, intramural forces are significantly greater and therefore best represented by the LV pressure multiplied by heart rate (LVRPP). In this study LV pressure was estimated from the echocardiographic peak AVG plus systolic blood pressure measured simultaneously by sphygmomanometry. All values are mean ± SD.

3. Results

3.1. LV dimensions, function and mass

All the subjects had septal and posterior wall thickness

greater than 12 mm (15 ± 2 mm) and severe aortic stenosis (peak AVG 89.2 ± 18.7 mmHg) at echocardiography.

Fifteen subjects fulfilled criteria for LVH with CMR [9] and all 20 had satisfactory left ventricular function, with an ejection fraction greater than 50% (table 1).

Table 1. CMR values for LV volumes, function and mass

End diastolic volume (ml)	113.6 ± 34.0
End systolic volume (ml)	35.6 ± 18.0
Stroke volume (ml)	77.9 ± 20.8
Ejection fraction (%)	69.9 ± 8.3
LV mass (g)	249.5 ± 52.3

3.2. Haemodynamics and MBF

As expected, during the PET studies heart rate increased from 63.6 ± 8.0 at rest to 80.2 ± 8.9 ($p < 0.00001$) during dipyridamole infusion. Systolic arterial pressure decreased from 132 ± 25 mmHg to 124 ± 23 mmHg ($p = 0.003$) during hyperaemia, whilst diastolic pressure remained constant (74 ± 10 at rest vs. 71 ± 11 during hyperaemia, $p = 0.14$).

Transmural (Tm), subendocardial (Endo), subepicardial (Epi) MBF values at baseline, during dipyridamole hyperaemia, and CVR are shown in table 2.

Table 2. PET values for MBF and CVR

	Baseline MBF (ml/min/g)	Hyperaemic MBF (ml/min/g)	CVR
Tm	1.05 ± 0.26	1.99 ± 0.78	1.90 ± 0.60
Endo	1.07 ± 0.24	1.94 ± 0.93	1.83 ± 0.79
Epi	0.98 ± 0.26	1.98 ± 0.73	2.02 ± 0.54

MBF was greater in the subendocardium than the subepicardium at baseline ($p = 0.003$) and comparable during hyperaemia. Under resting conditions the ventricular blood flow increased proportionally to LVM ($y = 0.99x + 15$; $r = 0.62$; $p = 0.004$), but the relationship was weaker during hyperaemia ($y = 1.65x + 83$; $r = 0.4$; p = ns). Transmural CVR was not correlated to LVM, as shown in figure 1.

Resting MBF was maintained within a constant range, independent of the intrinsic haemodynamic load of the ventricle (LVRPP) at baseline, whilst hyperaemic MBF was inversely related to LVRPP in both the subendocardium and subepicardium. Thus, LVRPP at rest and CVR were correlated by a logarithmic relationship in all three regions considered (figure 2), with CVR progressively decreasing as the LVRPP increased. This pattern was paralleled by the relationship between peak AVG at rest and CVR.

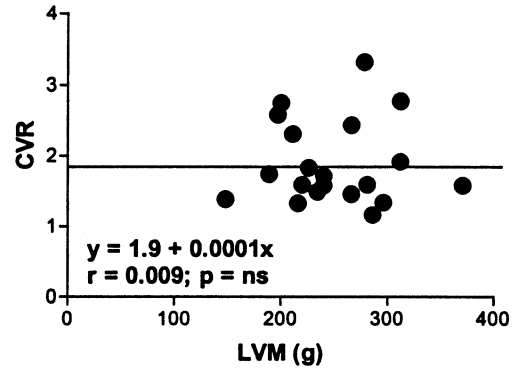

Figure 1. Relationship between transmural CVR and LVM.

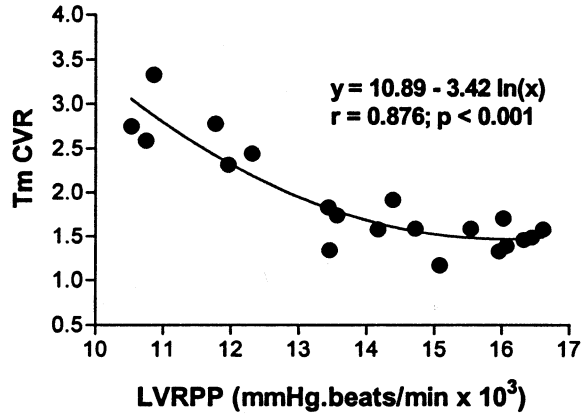

Figure 2. Graph of transmural CVR versus LVRPP

The peak AVG and LVRPP regression lines for the subendocardial and subepicardial CVR cross at 65.9 mmHg and 12.1×10^3 mmHg.beats/min respectively, suggesting that as peak AVG and LVRPP increase, a greater effect is exerted on the subendocardium than the subepicardium (figure 3).

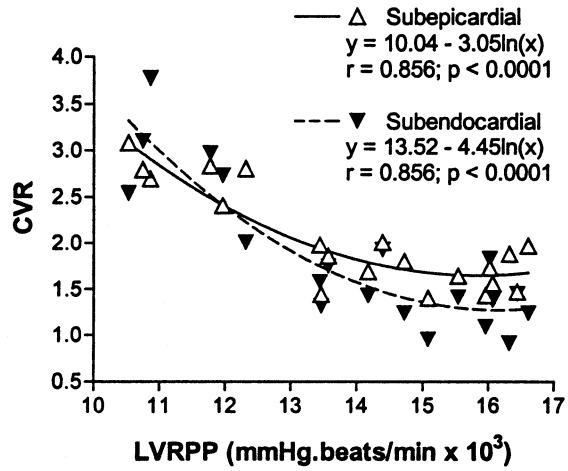

Figure 3. Graph of subendocardial & subepicardial CVR

versus LVRPP

4. Discussion

The CVR in the group of patients we studied was impaired, compared to that of matched normal subjects studied within our institution. [10] However, to date, the relative contribution of LVHand haemodynamic forces to the impairment of the coronary microvasculature was incompletely understood.

CMR provides accurate and reproducible assessment of LVM and, as proposed by the theory of autoregulation, ventricular blood flow increased proportionally with LVM, suggesting the increased oxygen demand of the hypertrophied myocardium at rest is met by an increase in basal blood flow. However, haemodynamic and intramural forces may oppose this action by a direct effect on the coronary microvasculature. These two opposing mechanisms may be responsible for maintenance of resting MBF within a constant range for varying haemodynamics, as demonstrated by normal values for each of the subjects, despite increasing peak AVG and LVRPP. This trend was demonstrated throughout the myocardium, including the subendocardial layer, which is most exposed to elevated LV pressures. This suggests a process of adaptation within the coronary microcirculation of the hypertrophied myocardium, maintaining an adequate blood supply for resting conditions. The CVR, however, showed no relationship with LVM, implying microcirculatory dysfunction is independent of the degree of myocyte hypertrophy. Conversely the relationship between peak AVG, or LVRPP, and the CVR demonstrated a blunting of the capacity for the microvasculature to subsequently respond to stress as haemodynamic forces increase. This appears to be at the expense of maintaining CVR for a range of left ventricular masses in the hypertrophied state. Again this was seen transmurally and not limited to a specific layer of myocardium, although at greater haemodynamic and intrinsic myocardial workloads, the subendocardial microcirculation appeared to be affected to a greater extent than the subepicardium, in agreement with previous data in animals. [11] Thus, in compensating for the increased baseline demand, the ability of the coronary microcirculation to respond to increased workload may be attenuated.

These findings suggest, as is often clinically apparent, that as the severity of the aortic stenosis increases, the haemodynamic effects exerted upon the myocardium and microcirculation eventually offset the compensation afforded by hypertrophy. This may have implications for surgical decision making, especially in otherwise asymptomatic patients.

Acknowledgements

This work was funded through a project grant (PG 98431) from the British Heart Foundation. KR is supported by a grant from the Hariri Foundation.

References

[1] Irvine T, Kenny A. Aortic stenosis and angina with normal coronary arteries: the role of coronary flow abnormalities. Heart 1997; 78(3):213-214.

[2] Choudhury L, Rosen SD, Patel D, Nihoyannopoulos P, Camici PG. Coronary vasodilator reserve in primary and secondary left ventricular hypertrophy. A study with positron emission tomography. Eur Heart J 1997; 18(1):108-116.

[3] Sheridan DJ. Left Ventricular Hypertrophy. First ed. London: Churchill Livingstone, 1998.

[4] Spinks TJ, Jones T, Bloomfield PM, Bailey DL, Miller M, Hogg D et al. Physical characteristics of the ECAT EXACT3D positron tomograph. Phys Med Biol 2000; 45:2601-2618.

[5] Schiller NB. Two-dimensional echocardiographic determination of left ventricular volume, systolic function, and mass. Summary and discussion of the 1989 recommendations of the American Society of Echocardiography. Circulation 1991; 84(3 Suppl):I280-I287.

[6] Currie PJ, Seward JB, Reeder GS, Vlietstra RE, Bresnahan, DR et al. Continuous-wave Doppler echocardiographic assessment of severity of calcific aortic stenosis: a simultaneous Doppler-catheter correlative study in 100 adult patients. Circulation 1985; 71(6):1162-1169.

[7] Bellenger NG, Francis JM, Davies LC, Coats ASJ, Pennell DJ. Establishment and performance of a magnetic resonance cardiac function clinic. J Cardiovasc Magn Reson 2, 15-22. 2000.

[8] Uren NG, Melin JA, de Bruyne B, Wijns W, Baudhuin T, Camici PG. Relation between myocardial blood flow and the severity of coronary-artery stenosis. N Engl J Med 1994; 330(25):1782-1788.

[9] Lorenz CH, Walker ES, Morgan VL, et al. Normal human right and left ventricular mass, systolic function, and gender differences by cine magnetic resonance imaging. J Cardiovasc Magn Reson 1999; 1:7-21.

[10] Chareonthaitawee P, Kaufmann P, Rimoldi O, Camici PG. Heterogeneity of resting and hyperemic myocardial blood flow in healthy humans. Cardiovasc Res 2001; In press.

[11] L'Abbate A, Marzilli M, Ballestra AM, Camici P, Trivella MG, Pelosi G et al. Opposite transmural gradients of coronary resistance and extravascular pressure in the working dog's heart. Cardiovasc Res 1980; 14(1):21-29.

Address for correspondence.

Dr Kim Rajappan MA MRCP
Academic Cardiology Unit
10th Floor QEQM Wing, St. Mary's Hospital
South Wharf Road, London, W2 1NY U.K.
kumaran.rajappan@ic.ac.uk